

MOL#38018

Title page

**Antithrombotic effect of a P-I Class Snake Venom Metalloproteinase, Kistomin,
is mediated by affecting Glycoprotein Ib-von Willbrand Factor Interaction**

Chun-Chieh Hsu, Wen-Bin Wu, Ya-Hui Chang, Heng-Lan Kuo and Tur-Fu Huang

Department of Pharmacology, College of Medicine, National Taiwan University,
Taipei, Taiwan (C.C.H., Y.H.C., H.L.K., T.F.H); School of Medicine, Fu-Jen Catholic
University, Taipei County, Taiwan (W.B.W.)

MOL#38018

Running Title page

Running Title: Venom Metalloproteinase Cleaves Platelet GPIb and vWF

Corresponding author: Tur-Fu Huang

Department of Pharmacology, College of Medicine, National Taiwan University,

No1, Sec1, Jen-Ai Rd, Taipei, Taiwan

Tel (886)-2-23562221

Fax (886)-2-23915602

E-mail: turfu@ntu.edu.tw

Number of text pages: 39

Number of tables: 2

Number of figures: 7

Number of reference: 25

Number of words in Abstract: 244

Number of words in Introduction: 422

Number of words in Discussion: 1144

ABBREVIATIONS: vWF, von Willebrand factor; SVMP, snake venom metalloproteinase; P-I~IV, protein-type I~IV; PRP, platelet-rich plasma; PS, platelet suspension; ADAMTS, a disintegrin and metalloproteinase with thrombospondin motifs; PSGL-1, P-selectin glycoprotein ligand-1.

MOL#38018

ABSTRACT

Binding of von Willebrand factor (vWF) to platelet glycoprotein (GP) Ib-IX-V mediates platelet activation in the early stage of thrombus formation. Kistomin, a snake venom metalloproteinase (SVMP) purified from venom of *Calloselasma rhodostoma*, has been shown to inhibit vWF-induced platelet aggregation. However, its action mechanism, structure-function relationship, and *in-vivo* antithrombotic effects are still largely unknown. In the present study, cDNA encoding kistomin precursor was cloned and revealed that kistomin is a P-I class SVMP with only a proteinase domain. Further analysis indicated that kistomin specifically inhibited vWF-induced platelet aggregation through binding and cleavage of platelet GPIb α and vWF. Cleavage of platelet GPIb α by kistomin resulted in release of 45- and 130-kDa soluble fragments, indicating kistomin cleaves GPIb α at two distinct sites. In parallel, cleavage of vWF by kistomin also resulted in the formation of low-molecular-mass multimers of vWF. In *ex-vivo* and *in-vivo* studies, kistomin cleaved platelet GPIb α in whole blood. Moreover, GPIb α agonist-induced platelet aggregation *ex vivo* was inhibited and tail-bleeding time was prolonged in mice intravenously administered with kistomin. Kistomin's *in-vivo* antithrombotic effect was also evidenced by prolonging the occlusion time in mesenteric microvessels of mice. In conclusion, kistomin, a P-I class metalloproteinase, has a relative specificity for GPIb α and vWF and its proteolytic activity on GPIb α -vWF is responsible for its antithrombotic activity both *in vitro* and *in vivo*. Kistomin can be useful as a tool for studying metalloproteinase-substrate interactions and has a potential being developed as an antithrombotic agent.

MOL#38018

Platelets play a key role in haemostasis and thrombosis. Exposure of subendothelial von Willebrand factor (vWF) is the first step to form thrombi to arrest blood loss at the sites of trauma, but abnormal embolism may also cause ischemia in pathogenic condition (Andrews and Berndt, 2004). The glycoprotein (GP) Ib complex, one of the major adhesive receptors expressed on platelets which interacts with vWF, is composed of GPIb α , GPIb β , GPIX and GPV. GPIb α consists of N-terminal flank, leucine-rich repeat, anionic sulfated tyrosine sequence, macroglycopeptide domain, transmembrane region and cytoplasmic tail (Andrews et al., 2003). Plasma vWF circulates primarily as dimer form and the multimeric forms of vWF are existed in the subendothelial matrix (Canobbio et al., 2004). It has been reported that Bernard-Soulier syndrome and platelet-type von Willebrand disease are inherited bleeding disorder due to mutations in GPIb complex and vWF gene, respectively, suggesting that GPIb-vWF interaction is very important for haemostasis. Therefore, modulation of the GPIb α -vWF interactions during thrombotic complications could be beneficial (Bonneffoy et al., 2003). However, in contrast to extensive application of α IIb β 3 antagonists during acute coronary diseases, no GPIb α -vWF axis inhibitor is commercially available, although some GPIb α or vWF antagonists are being preclinically developed.

MOL#38018

Snake venom proteases are invaluable tools for studying coagulation and haemostasis (Marsh, 2001). For examples, fibrinogen and antithrombin III can be assayed by using snake venom thrombin-like enzymes. Among these snake-derived proteases, snake venom metalloproteinases (SVMPs), which are abundant in *Viperidae* and *Crotalidae* venoms, are key enzymes responsible for local hemorrhage and are metal ion-dependent for their full function (Kamiguti, 2005; Matsui et al., 2000). The protein structural classification of SVMPs is presented as protein-type I (P-I) (having only metalloproteinase domain), P-II (having metalloproteinase and disintegrin domain), P-III (having metalloproteinase, disintegrin-like and cysteine-rich domain) and P-IV (having P-III structure plus lectin-like domains connected by disulfide bonds) (Fox and Serrano, 2005). It has been suggested that the additional disintegrin-like and the cysteine-rich regions domains may direct SVMP to its targets (Fox and Serrano, 2005). However, its structure-activity relationship remains unclear.

Kistomin, a 25-kDa SVMP purified from *Calloselasma rhodostoma* venom in our laboratory, has been shown to degrade fibrinogen and inhibits ristocetin-induced platelet agglutination, suggesting that it is a GPIb-cleaving protease (Huang et al., 1993). However, its action mechanism, structure-function relationship, and *in-vivo*

MOL#38018

antithrombotic effects are still largely unknown. In this study, cDNA-encoding kistomin was cloned and kistomin's cleaving and binding specificities for vWF and GP Iba were demonstrated. More importantly, kistomin's antithrombotic effect was examined in an *in-vivo* animal model.

MOL#38018

Materials and Methods

Materials. Anti-GPIIb α mAb M45 and SZ2, directed to the sulfated tyrosine residues of GPIIb α and inhibited ristocetin-dependent binding of vWF to GPIIb α , were obtained from CLB Immunoreagentia (Amsterdam, The Netherlands) and Immunotech (France), respectively. The murine mAb against $\alpha 2\beta 1$, 6F1, was kindly provided from Dr. Barry S. Coller (Mount Sinai School of Medicine, New York, NY). FITC-conjugated goat anti-mouse IgG was from Santa Cruz Biotechnology, Inc., USA. Heparin was from Fischers USA. Human purified vWF and fibrinogen were from Calbiochem, USA. Enhanced chemiluminescence (ECL) Western blotting system was from PerkinElmer Life Sciences (Boston, MA, USA). Other chemicals were purchased from Sigma Chemicals, Co. (St Louis, Mo, USA).

Venoms of *C. rhodostoma*, *C. atrox* and *T. flavoviridis* were from Latoxan (Rosans, France). Kistomin was purified from crude venom of *C. rhodostoma* as previously described (Huang et al., 1993), migrating as a single band at 25 kDa on SDS-PAGE assay. Crotalin (Wu et al., 2001b) and triflamp (Tseng et al., 2004a) were purified from *C. atrox* and *T. flavoviridis*, respectively.

Protein Sequencing of the Fragmented Kistomin and cDNA Cloning of

MOL#38018

Kistomin Precursor. Protein sequencing of the fragmented kistomin was performed as previously described (Wu et al., 2001a). Briefly, fragmented kistomin was obtained by alkylation with vinylpyridine and followed by incubation with CNBr. The fragments were applied to HPLC and the major fraction was subjected to protein sequencing. For sequencing of the autoproteolytic fragment of kistomin, kistomin was autoproteolyzed in 1% SDS and 0.5 M Tris-HCl solution, transblotted onto PVDF membrane and then analyzed by sequencing.

Total RNA was isolated from *C. rhodostoma* venom glands with a BlueExtract kit (LTK BioLaboratories Co., Ltd, Linko, Taipei, Taiwan). cDNA was synthesized from 1.5 mg of the total RNA and used to construct a cDNA library in the Uni-ZAP XR vector (Stratagene, La Jolla, CA, U.S.A.).

To obtain cDNA of putative SVMP, recombinant lambda DNA species were prepared from the cDNA library and used as templates in PCR. Primers for the first screening of cDNA library were 5'-TCCATCGAAGTC(G/A)TTGTT(G/A)AA-3' and 5'-TCAGGTTGG(C/T)TTGAAAGCAGG-3'. Amplification was performed by using Taq DNA polymerase (Ab peptides, St. Louis, USA) and the primers with a hot start at 94°C for 10 min and 30 cycles of denaturation (1 min, at 94°C), annealing (1 min, at 50°C), and extension (2 min, at 72°C). Primers for the second amplification of

MOL#38018

the 3'-end of the precursor cDNA of kistomin were 5'-GCGGATAAAAGCATGGTTGA-3' and M13 forward primer. PCR was performed at the same condition except primer-annealing temperature was set at 45 °C. The final PCR products were analyzed by 1% (w/v) agarose-gel electrophoresis and purified by electroelution. The purified DNA fragments were ligated to pcRII-TOPO vector with a TA cloning kit (Invitrogen, Carlsbad, CA, U.S.A.) and sequence analysis was performed. The specificity of the second amplification was confirmed from the overlapping sequences that were distinguishable from the other SVMs. Sequences were assembled with the GCG program (Wisconsin Package version 10.1, Genetics Computer Group).

Platelet Aggregation. Blood was collected from healthy human volunteers and anticoagulated with 3.8% sodium citrate (9:1, v/v). Citrated blood was immediately centrifuged for 10 min at 120 g and 25°C, and the supernatant (platelet-rich plasma, PRP) was obtained. Human washed platelet suspension (PS) was prepared as previously described (Liu et al., 1996) and adjusted to about 3.8×10^8 platelets/ml. Platelet aggregation was monitored by light transmission in a Lumi-Aggregometer (Chrono-Log, Havertown, PA) with continuous stirring at 900 rpm at 37°C as

MOL#38018

previously described (Liu et al., 1996).

For *ex vivo* assay of mouse platelet aggregation, male ICR mice (12-15 g) were intravenously injected with different dosage of kistomin. After 20 min, mouse was anesthetized with sodium pentobarbital (50 µg/g, ip) and blood was collected by cardiac puncture. PRP was obtained by centrifugation at 200 g for 4 min at room temperature. After washing twice with Tyrodes' solution, platelet suspension was adjusted to about 5×10^8 platelets/ml and aggregation was measured turbidimetrically.

Flow cytometric analysis of platelet receptor expression. Washed human platelets were prepared as described above. PS (3.8×10^8 platelets/ml) containing 2 µM PGE₁ was incubated with kistomin 20 µg/ml at 37°C for 10 min. After an extensive wash, platelets were labeled with mAb against GPIbα (SZ2), αIIbβ3 (7E3) or α2β3 integrin (6F1) at room temperature (RT) for 30 min. Labeled cells were washed with Tyrodes' solution and then incubated with secondary FITC-conjugated goat antimouse IgG (CALTAG Lab, Burlingame, CA) RT for 30 min with a continuous shaking. After incubation, cells were washed, resuspended in PBS, and analyzed immediately by FACS Calibur (Becton Dickinson, USA).

MOL#38018

Western Blot Analysis of Platelet GPIb α . Platelet suspension was centrifuged at 200 g for 5 min. After removing of the supernatant, pellets were lysed by 1% triton buffer (in PBS). Aliquots of cell lysates and supernatants were resolved on 10% SDS-PAGE under reducing conditions and electrotransferred to Immobilon-PVDF membrane (Millipore). After blocking in a 0.5% BSA in Tri-buffered saline 1 hr at 4°C, the blots were probed with anti-GP Ib α mAb (1:1000) for overnight at 4°C and followed by the horseradish peroxidase-goat anti-mouse IgG. The protein was visualized by adding of enhanced chemiluminescence (ECL) solution (Pierce, US).

Determination of kistomin binding to platelet GPIb α . For determination of the interaction between kistomin and GPIb α , flowcytometric and Western blot analysis were performed. For flowcytometry, platelets were incubated with or without kistomin at 4 °C and followed by probing with FITC-conjugated anti-GPIb α mAb, M45. Cells were analyzed immediately by FACS Calibur (Becton Dickinson, USA). For western blot analysis, kistomin (20 μ g) and agglucetin (15 μ g) were applied to 15% SDS-PAGE and transferred on to a PVDF membrane. Platelets lysate was obtained by lysis of platelet pellet in lysis buffer (10 mM HEPES buffer containing 10% SDS, 10mM *N*-ethylmaleimide, 20 mM Na₃VO₄, 20mM EDTA, 10 mM

MOL#38018

phenylmethylsulfonyl fluoride). The membrane was blocked with 1% BSA and then incubated with platelet lysate for 1 hr at RT. After a brief wash, the membrane was probed with anti-GPIIb α SZ2 mAb and developed by ECL.

Cleavage of vWF by Kistomin. Purified human vWF (1.5 μ g) incubated with or without kistomin were analyzed as previously described (Wu et al., 2001b) with a minor modification. Briefly, aliquots of the mixture were analyzed by SDS-1% agarose gel electrophoresis (~2 mm) in a Mupid-2 Mini-Gel system (Cosmo Bio Co., LTD, Tokyo, Japan) and electroblotted onto PVDF membrane. Immunoblots were developed with peroxidase-conjugated antihuman vWF antibody (Dakopatts, Glostrup, Denmark).

Fluorescent Dye-induced Platelet Thrombus Formation in Mesenteric Microvessels of Mice. Fluorescent dye-induced platelet thrombus formation in mesenteric microvessels of mice was performed as previously described (Chang and Huang, 1994) with some modifications. Briefly, after male ICR mice (12-15 g) were anesthetized with sodium pentobarbital (50 μ g/g, ip), fluorescein sodium (12.5 μ g/g) was intravenously injected. A segment of small intestine attached to its mesentery was

MOL#38018

loosely exteriorized for microscopic observation. Venules with diameters of 30 to 40 μm were selected to produce a microthrombus. In the epi-illumination system, the area of irradiation (wavelength above 520 nm) was about 50 μm in diameter on the focal plane. After the operation (15 min), the mouse was intravenously injected with PBS (control, 30 μl), aspirin or kistomin through another lateral tail vein of the mouse. Five min after administration of these drugs, the irradiation by filtered light and the occlusion time was recorded.

Tail Bleeding Time. After anesthesia with sodium pentobarbital (50 $\mu\text{g/g}$, ip), male ICR mice (12-15 g) were intravenously injected with phosphate buffer saline (PBS, vehicle, 30 μl), aspirin or kistomin through a lateral tail vein. After 5 min, the mouse was placed in a tube holder with its tail protruding and then a cut 2 mm from the tail tip was made. Immediately, the tail was vertically immersed into normal saline at 37°C. Bleeding time was recorded from the time bleeding started till it completely stopped.

MOL#38018

Results

Protein Sequencing and cDNA Cloning of Kistomin. To have an insight on kistomin's primary structure, protein sequencing was performed. A 14-kDa autoproteolytic fragment from kistomin was sequenced and its N-terminal was revealed as LSKRKPHNDAQFLTNDKDFDG (fragment 1). Moreover, two peptide sequences, VDKHNGNIKKIE (fragment 2) and APEVNNNPTKKFSDC (fragment 3), were obtained from CNBr digestion of kistomin.

To further determine the cDNA sequence of kistomin precursor, cDNA cloning was performed. Two primers in accordance with the conserved PKMCGV sequence of SVMP and the autoproteolytic fragment were used in the first amplification of kistomin cDNA. After screening of *C. rhodostoma* cDNA library, a clone with about ~900 bp was obtained, representing the kistomin precursor presequence containing the partial metalloproteinase domain of kistomin (data not shown). To obtain the remaining cDNA sequence of kistomin, a pair of primers according to the sequences from kistomin-CNBr-digested fragment (VDKHNGNIKKIE) and vector was used. Fig. 1 showed the assembled cDNA sequence and the deduced amino acid sequence of the kistomin precursor. Three partial sequences obtained from direct protein sequencing were found in the deduced amino acid sequence with 100% identity (Fig.

MOL#38018

1, underlined sequences), indicating that it is a kistomin precursor. The precursor, designated prokistomin, consists of a presequence, prosequence and a metalloproteinase domain and belongs to a P-I SVMP. A putative start site was indicated and mature kistomin predicted from this site was 227 residues (Fig. 1), which was estimated to be 25.7 kDa. The deduced a.a. sequence of prokistomin contains the characteristic zinc-chelating sequence, HEIGHN¹LGMEHD (Fig. 1, catalytic site), which is similar to that of other SVMPs, such as fibrolase (Randolph et al., 1992) and jararhagin (Paine et al., 1992).

Kistomin Inhibits Ristocetin-induced Platelet Agglutination and Aggregation. To reexamine kistomin's activity in inhibiting platelet function, platelet suspension (PS) agglutination and platelet-rich plasma (PRP) aggregation were performed. As shown in Fig. 2, kistomin concentration-dependently inhibited ristocetin-induced platelet agglutination and aggregation with a half-maximal inhibition concentration (IC₅₀) at 2.04 µg/ml (0.079 µM) and 8.25 µg/ml (0.321 µM), respectively. However, this inhibition was abolished by the treatment of kistomin with EDTA or o-phenanthroline (data not shown), indicating the involvement of an enzymatic reaction.

MOL#38018

Kistomin Cleaves Platelet GPIb α . To further elucidate the possible action mechanism of kistomin in inhibiting ristocetin-induced platelet aggregation, GPIb α expression on platelets was analyzed by flow cytometry and Western blotting. As depicted in immunofluorescence staining with anti-GPIb α mAb SZ2, kistomin treatment rapidly reduced the level of GPIb α expression on platelets, whereas the expression of the other two important platelet receptors, namely α IIB β 3 and α 2 β 1 integrins, were not affected (Fig. 3A).

To characterize the proteolytic properties of kistomin on platelet GPIb α , Western blotting was performed. It was found that platelet intact GPIb α (~140 kDa) was cleaved by kistomin in a time-dependent manner, which could be abolished by EDTA (Fig. 3B). One intact GPIb α and two fragments migrated at molecular masses of ~140 kDa, ~130 kDa and ~45 kDa, respectively, were detected by anti-GPIb α SZ2 mAb in total platelet lysate (arrows). Surprisingly, only two fragments (~130 kDa and ~45 kDa) were detected in supernatant (Fig. 3C), indicating that kistomin cleaves platelet GPIb α at two distinct sites to generate two soluble fragments, which can be recognized by the SZ2 mAb.

Binding of Kistomin to GPIb α . Since platelet GPIb α was cleaved by kistomin,

MOL#38018

we next investigated whether kistomin bound to GPIb α . To stop kistomin's enzymatic activity, the experiment was performed at 4°C. Under this condition, kistomin bound to GPIb α and replaced anti-GPIb α M45 mAb binding to platelets in a concentration-dependent manner (Fig. 4A). Binding of kistomin to GPIb α concentration-dependently increased and reached saturation at the concentrations more than 20 μ g/ml (Fig. 4B). This result was confirmed by the observation that immobilized kistomin directly interacted with GPIb α in platelet lysate. Interestingly, this binding was not affected in the presence of EDTA (Fig. 4C), suggesting that bivalent cations are not required in this interaction. A similar binding ability was also found in immobilized agglucetin, a tetrameric GPIb α -binding protein from *A. acutus* (Wang and Huang, 2001), in which it migrated as two distinct bands at 16.2 and 14.5 kDa (Fig. 4, lane 3). In contrast, rhodostomin, an RGD-containing disintegrin purified from *C. rhodostoma* venom (Huang et al., 1990), failed to bind platelet GPIb α (data not shown).

Effect of Kistomin on the Multimeric Structure of vWF. We have shown that kistomin could bind and cleave platelet GPIb α (Fig. 3 and 4). To further examine whether kistomin affected multimeric structure of vWF, human vWF preincubated with or without kistomin was added to platelet suspension and ristocetin-induced

MOL#38018

platelet agglutination was measured. Fig. 5A showed that ristocetin-induced agglutination was time-dependently reduced under this condition but almost fully restored by re-adding a new intact vWF. Further analysis revealed that high-molecular-mass multimers of vWF obviously decreased and concomitantly the low-molecular-mass multimers increased in the presence of kistomin (Fig. 5B, lanes 1 and 2). Again, the cleavage of vWF by kistomin was abolished in the presence of EDTA or o-phenanthroline (Fig. 5B, lanes 3 and 4). Taken together, our results indicate that kistomin can bind and cleave platelet GPIb α and vWF and subsequently inhibits vWF-induced platelet agglutination and aggregation.

Kistomin Affects Thrombosis and Haemostasis *In Vivo*. We next investigated whether kistomin exerted antithrombotic effect *in vivo*. It was shown that kistomin potently decreased Ab binding to platelet GPIb α in human whole blood, whereas crotalin and triflamp, two P-I SVMPs purified from venom of *C. atrox* (Wu et al., 2001b) and *T. flavoviridis* (Tseng et al., 2004a), respectively, were less effective at the same concentration in cleaving GPIb α (Fig. 6). We therefore hypothesized that kistomin could be an active protease both in *in-vitro* and *in-vivo* condition. To confirm this hypothesis, we measured *ex-vivo* platelet aggregation in PRP or PS

MOL#38018

prepared from kistomin-pretreated mouse. Because ristocetin is ineffective in causing platelet aggregation in mouse PRP, a snake venom-derived GPIIb/IIIa agonist, gramicetin, was used in this assay (Wu et al., 2001a). As shown in Fig. 7A, gramicetin-induced platelet agglutination was inhibited by the GPIIb/IIIa antagonist, agkistatin, suggesting that a GPIIb/IIIa-mediated pathway was involved in this agglutination. The agglutination was suppressed in PRP prepared from mouse treated with kistomin (Fig. 7B), however, collagen-, ADP-, convulxin- and thrombin-induced platelet aggregation was not significantly affected (Fig. 7C-F). Thus, kistomin impaired mouse platelet function specifically through affecting GPIIb/IIIa *in vivo*.

We then determined kistomin's antithrombotic effects *in vivo*. In fluorescent dye-treated mice, thrombus formation was observed in irradiated mesenteric venules of mice. The occlusion time of irradiated vessels was 134.3 ± 6.2 s in control mice (n=12) but was prolonged to 173.2 ± 26.7 s (n=13) and 301.9 ± 43.5 s (n=10) by aspirin at doses of 150 and 250 $\mu\text{g/g}$, respectively. Surprisingly, in comparison with aspirin, kistomin also exerted potent antithrombotic effect *in vivo*, prolonging the occlusion time to 194.9 ± 12.5 s (n=10) and 273.2 ± 16.2 s (n=10) at doses of 1.5 and 7 $\mu\text{g/g}$, respectively (Table 1). Kistomin was approximately 4,000-fold more potent than aspirin in prolonging microvessel occlusion time on a molar basis. In parallel, the

MOL#38018

tail bleeding time of mice (control, 90.8 ± 5.0 s, n=17) was prolonged to 172.1 ± 26.3 s and more than 1800 s by kistomin at the given doses of 1.5 and 7 $\mu\text{g/g}$, respectively. In contrast, aspirin at 150 and 250 $\mu\text{g/g}$ also increased bleeding time to 559 ± 48.9 s (n=13) and more than 1800 s (n=10), respectively (Table 2).

MOL#38018

Discussion

Platelet GPIb α -vWF interaction has been identified as an important target for therapeutics to prevent ischemic cardiovascular events (Jackson and Schoenwaelder, 2003). We formerly found that kistomin inhibited ristocetin-induced platelet agglutination in platelet suspension (Huang et al., 1993), however its action mechanism, antithrombotic activity and structure-activity relationship are still largely unknown. In this study, we demonstrated that kistomin is capable of binding to platelet GPIb α and cleaves GPIb α and vWF, exhibiting potent antiplatelet and antithrombotic activities *in vitro* and *in vivo*. More importantly, cDNA encoding kistomin precursor was cloned and revealed that mature kistomin is a P-I SVMP with only a metalloproteinase domain. The sequence of kistomin is shown with 51% identity to the P-I SVMP fibrolase, a fibrinolytic enzyme from *Agkistrodon contortrix contortrix* venom (Randolph et al., 1992), and with 40% identity to the P-III SVMP jararhagin, an α 2 β 1- and vWF-cleavage protease from *Bothrops jararaca* venom (Paine et al., 1992). Moreover, kistomin shares 29% identity with the proteinase domain of human ADAMTS13 (a disintegrin and metalloproteinase with thrombospondin motifs 13), an endogenous metalloproteinase specifically cleaving between Tyr842 and Met843 in the A2 domain of vWF to regulate its physiological

MOL#38018

haemostatic activity (Levy et al., 2001). Being a P-I SVMP without an additional disintegrin/cysteine-rich domain, kistomin still has a relative strong selectivity toward platelet GPIb α and vWF, suggesting that the additional domain(s) are(is) not necessarily required for the substrate recognition. From the protein chemistry and evolutionary viewpoint, it is an interesting issue to know why these SMVPs and matrix metalloproteases have a similar specificity for GPIb α and/or vWF.

Kistomin inhibits vWF-induced platelet agglutination and aggregation through acting on platelet GPIb α and vWF. Several lines of evidence indicate that the platelet GPIb α and vWF were cleaved by kistomin during their coincubation. First of all, a significantly reduced binding signal in flowcytometry was observed after platelets were treated with kistomin (Fig. 3A). Secondly, outer membrane portion of GPIb α was cleaved from platelet membrane into supernatant in the presence of kistomin and generated two soluble fragments, which migrated at the molecular masses of 45- and 130-kDa (Fig. 3, B and C). Thirdly, kistomin competitively inhibited anti-GPIb α mAb interaction with platelet and directly bound to platelet GPIb α , as determined by flowcytometry and Western blotting (Fig. 4). Fourthly, vWF-induced platelet agglutination was compromised by a preincubation of vWF with kistomin but reversed by adding an intact vWF (Fig. 5A). Fifthly, upon kistomin incubation, high

MOL#38018

molecular mass multimers of vWF generated low molecular mass multimers (Fig. 5B). Lastly, EDTA pretreatment can abolish these activities of kistomin (Fig. 3, 5 and data not shown), indicating kistomin is a typical SVMP, mediating antiplatelet activities through cleaving GPIb α and vWF.

Regarding specificity, the surface marker analysis showed that kistomin failed to affect the binding of anti- α 2 β 1 (6F1) and α IIB β 3 (7E3) mAbs to platelets. In contrast, kistomin specifically inhibited the binding of anti-GPIb α mAbs to platelets, including AP1, 6D1 and SZ2 (Fig. 3A and data not shown). Moreover, platelets, prepared from kistomin-treated mice, were unable to agglutinate in response to GPIb α -agonist induction, but were able to aggregate in response to other agonists (Fig. 7), suggesting its relative specificity toward GPIb α both *in vitro* and *in vivo*. The GPIb α -binding epitopes for 6D1 and AP1 have been demonstrated to be located at the amino acid residues 104-128 and 201-268, respectively (Coller et al., 1983). SZ2 mAb has been shown to recognize anionic sulfated tyrosine residues 269 to 282 of GPIb α (Ward et al., 1996). Therefore, failed binding of these Abs to platelet in the presence of kistomin indicates that kistomin may cleave GPIb α downstreaming the anionic tyrosine sulfated region. In Fig. 3, we found that outer membrane portion of GPIb α was cleaved by kistomin to generate a ~130 kDa soluble fragment. Since it was a

MOL#38018

soluble fragment found in total cell lysate and in the supernatant (Fig. 3C), the possibility of cleavage of GPIb α at the site near N-terminus was excluded. Therefore, the first cleavage site was hypothesized to be located near C-terminus of GP Ib α . The cytoplasmic tail of GPIb α contains 96 amino acid residues (Berndt et al., 2001) and is estimated to have molecular mass of about 10 kDa. Therefore, the first cleavage site on GPIb α may be located near the outer membrane of platelet. Secondly, a ~45kDa soluble fragment increased gradually accompanying with a decrease of the ~130kDa fragment (Fig. 3), suggesting kistomin's second cleavage site is located within the ~130 kDa GPIb α fragment. This is evidenced by the observations that inactivated kistomin competitively replaced the binding of anti-GPIb α M45 mAb, which recognizes anionic sulfated tyrosine residues of GPIb α (Fig. 4). Kistomin seems to act like mocarhagin, a P-III SVMP, by cleaving GPIb α at a single site between Glu282 and Asp283 to generate a ~40 kDa fragment. However, this ~45kDa fragment could be recognized by SZ2 on Western blotting analysis (Fig. 3B and C), indicating that the binding epitope of SZ2, anionic sulfated tyrosine residues of GPIb α , still remained on the fragment. According to the size of the second fragment (~45kDa) and the binding epitopes of anti-GPIb α mAbs (SZ2 and M45), we postulated that the second kistomin-cleavage site on GPIb α is near downstream of the anionic sulfated

MOL#38018

tyrosine region. Taken together, we suggest that kistomin cleaves GPIb α at two distinct sites, one of which locates at the region near the outer membrane and another locates near anionic sulfated tyrosine. Kistomin's exact cleavage sites on GPIb α are still under investigation in our laboratory.

Our study also demonstrated that kistomin potently cleaved platelet GPIb α in human whole blood, as compared with crotalin and triflamp, two P-I SVMPs (Fig. 6). It has been shown that human α 2-macroglobulin and mouse macroglobulin are abundant in serum and capable of inhibiting and neutralizing the proteolytic activity of most proteinases, including some SVMPs (Tseng et al., 2004b). However, in this report, kistomin was demonstrated to elicit its antiplatelet and antithrombotic *in vivo* (Fig. 7 and Table 1 and 2). These suggest that kistomin is less susceptible to be neutralized by globulins in serum and possibly can be developed as an antithrombotic agent. This is supported by the data shown in Table 1 and 2, in which aspirin (150 μ g/g) and kistomin both delayed the irradiation-induced occlusion time to a similar degree, but kistomin appears to be safer at a lower dose (1.5 μ g/g) than aspirin in causing bleeding.

In conclusion, in this report we demonstrated that a P-I SVMP, kistomin, blocked vWF-induced platelet activation by specifically cleaving platelet GPIb α and

MOL#38018

vWF, suggesting that a metalloproteinase without an additional disintegrin/cysteine-rich domain has a relative specificity for GPIIb α and vWF. More importantly, kistomin exerted an antithrombotic effect *in vivo* with certain properties quite different from those of P-I SVMPs derived from other snake venoms. Therefore, kistomin may be useful as a tool for studying the function of vWF-GPIIb α , providing an alternative approach for the designing of antithrombotic agents.

MOL#38018

Acknowledgments

We appreciate the generous supply of mAbs from Dr. B.S. Coller (7E3, 6D1, and 6F1) and Dr. R.R. Montgomery (AP1). We also thank Dr. L.P. Chow for protein sequencing.

MOL#38018

References

- Andrews RK and Berndt MC (2004) Platelet physiology and thrombosis. *Thromb Res* 114:447-453
- Andrews RK, Gardiner EE, Shen Y, Whisstock JC and Berndt MC (2003) Glycoprotein Ib-IX-V. *Int J Biochem Cell Biol* 35:1170-1174
- Berndt MC, Shen Y, Dopheide SM, Gardiner EE and Andrews RK (2001) The vascular biology of the glycoprotein Ib-IX-V complex. *Thromb Haemost* 86:178-188
- Bonneffoy A, Vermeylen J and Hoylaerts MF (2003) Inhibition of von Willebrand factor-GPIb/IX/V interactions as a strategy to prevent arterial thrombosis. *Expert Rev Cardiovasc Ther* 1:257-269
- Canobbio I, Balduini C and Torti M (2004) Signalling through the platelet glycoprotein Ib-V-IX complex. *Cell Signal* 16:1329-1344
- Chang MC and Huang TF (1994) In vivo effect of a thrombin-like enzyme on platelet plug formation induced in mesenteric microvessels of mice. *Thromb Res* 73:31-38
- Coller BS, Peerschke EI, Scudder LE and Sullivan CA (1983) Studies with a murine monoclonal antibody that abolishes ristocetin-induced binding of von Willebrand factor to platelets: additional evidence in support of GPIb as a platelet receptor for

MOL#38018

von Willebrand factor. *Blood* 61:99-110

Fox JW and Serrano SMT (2005) Structural considerations of the snake venom metalloproteinases, key members of the M12 reprotolysin family of metalloproteinases. *Toxicon* 45:969-985

Huang TF, Chang MC and Teng CM (1993) Antiplatelet protease, kistomin, selectively cleaves human platelet glycoprotein Ib. *Biochim Biophys Acta* 1158:293-299

Huang TF, Chang MC, Peng HC and Teng CM (1992) A novel alpha-type fibrinogenase from Agkistrodon rhodostoma snake venom. *Biochim Biophys Acta* 1160:262-268

<Huang TF, Ouyang C and Teng CM (1990) Abstract 141, XIth International Congress on Thrombosis, Ljubljana, Yugoslavia.>

Jackson SP and Schoenwaelder SM (2003) Antiplatelet therapy: in search of the 'magic bullet'. *Nat Rev Drug Discov* 2:775-789

Kamiguti AS (2005) Platelets as targets of snake venom metalloproteinases. *Toxicon* 45:1041-1049

Levy GG, Nichols WC, Lian EC, Foroud T, McClintick JN, McGee BM, Yang AY, Siemieniak DR, Stark KR, Gruppo R, Sarode R, Shurin SB, Chandrasekaran V,

MOL#38018

- Stabler SP, Sabio H, Bouhassira EE, Upshaw JD Jr, Ginsburg D and Tsai H (2001) Mutations in a member of the ADAMTS gene family cause thrombotic thrombocytopenic purpura. *Nature* 413:488-494
- Liu CZ, Hur BT and Huang TF (1996) Measurement of glycoprotein IIb/IIIa blockade by flow cytometry with fluorescein isothiocyanate-conjugated crotavirin, a member of disintegrins. *Thromb Haemost* 76:585-591
- Marsh NA (2001) Diagnostic Uses of Snake Venom. *Haemostasis* 31:211-217
- Matsui T, Fujimura Y and Titani K (2000) Snake venom proteases affecting hemostasis and thrombosis. *Biochim Biophys Acta* 1477:146-156
- Paine MJ, Desmond HP, Theakston RD and Crampton JM (1992) Purification, cloning, and molecular characterization of a high molecular weight hemorrhagic metalloprotease, jararhagin, from *Bothrops jararaca* venom. Insights into the disintegrin gene family. *J Biol Chem* 267:22869-22876
- Randolph A, Chamberlain SH, Chu HLC, Retzios AD, Markland FS Jr and Masiarz FR (1992) Amino acid sequence of fibrolase, a direct-acting fibrinolytic enzyme from *Agkistrodon contortrix contortrix* venom. *Protein Sci* 1:590-600
- Tseng YL, Lee CJ and Huang TF (2004a) Effects of a snake venom metalloproteinase, trflamp, on platelet aggregation, platelet-neutrophil and neutrophil-neutrophil

MOL#38018

interactions: involvement of platelet GPIIb/IIIa and neutrophil PSGL-1. *Thromb Haemost* 91:315-324

Tseng YL, Wu WB, Hsu CC, Peng HC and Huang TF (2004b) Inhibitory effects of human alpha2-macroglobulin and mouse serum on the PSGL-1 and glycoprotein Ib proteolysis by a snake venom metalloproteinase, trypsin. *Toxicon* 43:769-777

Wang WJ and Huang TF (2001) A novel tetrameric venom protein, agglutinin from *Agkistrodon acutus*, acts as a glycoprotein Ib agonist. *Thromb Haemost* 86:1077-1086

Ward CM, Andrews RK, Smith AI and Berndt MC (1996) Mocarhagin, a novel cobra venom metalloproteinase, cleaves the platelet von Willebrand factor receptor glycoprotein Iba/IIb. Identification of the sulfated tyrosine/anionic sequence Tyr-276-Glu-282 of glycoprotein Iba/IIb as a binding site for von Willebrand factor and alpha-thrombin. *Biochemistry* 35:4929-4938

Wu WB, Chang SC, Liao MY and Huang TF (2001a) Purification, molecular cloning and mechanism of action of graminelysin I, a snake-venom-derived metalloproteinase that induces apoptosis of human endothelial cells. *Biochem J* 357:719-728

Wu WB, Peng HC and Huang TF (2001b) Crotalin, a vWF and GPIIb cleaving

MOL#38018

metalloproteinase from venom of *Crotalus atrox*. *Thromb Haemost* **86**:1501-1511

MOL#38018

Footnote

This work was financially supported by grants from the National Science Council,
Taiwan.

MOL#38018

Legends of Figures

Fig. 1. cDNA sequence and deduced amino acid sequence of the putative protein precursor of kistomin. The sequence shown begins with the presequence, and the translation stop codon is indicated by an asterisk (*). Three fragments from CNBr-digested and autoproteolytic kistomin are indicated by underlines.

Fig. 2. Effect of kistomin on ristocetin-induced platelet agglutination and aggregation. (A) Washed platelet suspension (PS) and (B) platelet-rich plasma (PRP) were pretreated with various concentrations of kistomin prior to the addition of ristocetin (1 mg/ml, arrow). Platelet agglutination and aggregation were monitored by turbidimetry in aggregometer. (C and D). Quantitative analysis of the data from (A) (B) and similar experiments were performed. Data were presented as percentage of control and were mean \pm SEM ($n \geq 3$).

Fig. 3. Effect of kistomin on platelet GPIb α . (A) Flow cytometric analysis of GPIb α expression on platelets. Washed platelets treated with PBS (gray area) or kistomin (5 μ g/ml, open area) at 37°C for 10 min were incubated with anti-GPIb α (SZ2), anti- α IIB β 3 (7E3) or anti- α 2 β 1 (6F1) mAbs and subjected to be analyzed by

MOL#38018

flowcytometry. (B, C) Western blot analysis of GPIb α expression on platelets. Washed platelets were treated with kistomin (20 μ g/ml) at 37°C for (B) different duration as indicated or (C) for 30 min in the absence or presence of EDTA. Total cell lysates, cells pellets (P) and supernatant (S) were obtained as described in *Materials and Methods* and analyzed by Western blotting. An arrowhead indicates an intact GPIb α expression on platelet. Note that a 130-kDa (open arrowheads) and a 45-kDa fragment (arrows) were observed in (B) total cell lysates and in (C) the supernatant of kistomin-treated platelets. This experiment is a representative of at least three similar experiments.

Fig. 4. Kistomin binds to platelet GP Ib α . (A) Kistomin competitively replaced anti-GPIb α mAb binding to platelets. Human washed platelets were incubated with PBS (gray area) or various concentrations of kistomin (open areas, 15, 30, and 60 μ g/ml) at 4°C for 30 min, followed by incubation with FITC-conjugated anti-GPIb α mAb, M45, and then analyzed by flowcytometry. The histogram was representative from three similar experiments. (B) Quantitative analysis of binding assay data from (A) and similar experiments were performed. Data were expressed as mean fluorescence and were mean \pm S.E. (n=3) (C) Platelet GPIb α bound to immobilized

MOL#38018

kistomin. Kistomin (Kis, 20 μ g) pretreated with vehicle or EDTA (10 mM) and agglucetin (agg, 15 μ g) were applied to SDS-PAGE and transferred to PVDF membrane. The membrane was incubated with platelet total lysate and followed by Western blot analysis using anti-GPIb α mAb, SZ2. This experiment is a representative one of at least three similar experiments.

Fig. 5. Effect of kistomin on the multimeric structure of vWF. (A) Pretreatment of vWF with kistomin compromised vWF-induced platelet aggregation. Washed human platelets was incubated with kistomin (3 μ g/ml)-pretreated vWF (10 μ g/ml) at 37°C for the indicated times and ristocetin (ris, 1 mg/ml) was added to induce platelet aggregation. In the case of prior coincubation of vWF and kistomin for 20 min, intact vWF (10 μ g/ml, arrow) was re-added 3 min after addition of ristocetin. (B) Kistomin cleaved the multimeric structure of vWF. Human vWF (0.5 μ g) was incubated at 37°C for 30 min with PBS (lane 1), kistomin (15 μ g/ml, lane 2), EDTA (10 mM)-treated kistomin (lane 3) or o-phenanthroline (10 mM)-treated kistomin (lane 4). Aliquots of each reaction mixture were subjected to SDS-1% agarose electrophoresis and vWF multimer were detected by peroxidase-conjugated anti-vWF antibody after blotting to a PVDF membrane. This experiment is a representative one of at least three similar

MOL#38018

experiments.

Fig. 6. Kistomin cleaves GPIb α in whole blood. Human whole blood was pretreated with PBS (gray area) and the indicated SVMPs (open areas, 100 μ g/ml for each) at 37°C for 15 min. Samples were probed by FITC-conjugated anti-GPIb α M45 Ab and immediately analyzed by flowcytometry. This experiment is a representative of at least three similar experiments.

Fig. 7. *Ex vivo* test regarding the effects of kistomin on mouse platelets. (A) GP Ib α antagonist inhibited gramicetin-induced platelet agglutination. Mouse PRP was treated with PBS or agkistin (5 μ g/ml) and platelet agglutination was induced by adding gramicetin (1 μ g/ml, solid arrow). (B) PRP was prepared from mice treated with vehicle or the indicated doses of kistomin and gramicetin-induced platelet agglutination was measured by aggregometry. (C-E) PRP or PS (F) was prepared from mice treated with vehicle or kistomin (kis, 7 μ g/g). Induction of platelet aggregation was done by adding collagen (10 μ g/ml), ADP (20 μ M), convulxin (cvx, 1.5 μ g/ml) and thrombin (0.1 U) and was measured by aggregometry. This experiment is a representative of at least three similar experiments.

MOL#38018

Tables

Table 1

Effect of kistomin on fluorescent dye-induced platelet-rich thrombus
formation in mesenteric venules of mice

| | | Occlusion time (s) | n |
|---------------|----------|--------------------|----|
| Control (PBS) | | 134.3 ± 6.2 | 12 |
| Aspirin | 150 µg/g | 172.6 ± 6.3*** | 16 |
| | 250 µg/g | 287.4 ± 15.2*** | 13 |
| Kistomin | 1.5 µg/g | 194.9 ± 12.5*** | 10 |
| | 7 µg/g | 273.2 ± 16.2*** | 10 |

Values are presented as means ± SEM of experimental number (n)

indicated. *** $p < 0.001$ as compared with control.

MOL#38018

Table 2

Effect of kistomin on the tail bleeding time of mice

| | | Tail bleeding time (s) | n |
|---------------|----------|------------------------|----|
| Control (PBS) | | 90.8 ± 5.1 | 17 |
| Aspirin | 150 µg/g | 559.0 ± 48.9*** | 15 |
| | 250 µg/g | >1800.0*** | 15 |
| Kistomin | 1.5 µg/g | 172.1 ± 26.3** | 17 |
| | 7 µg/g | >1800.0*** | 13 |

Values are presented as means ± SEM of experimental number (n)

indicated. **P<0.01 as compared with control. ***P<0.001 as

compared with control.

| | | |
|------|---|-------------|
| 1 | ATGATTGAGGTTCTCTTGGTGACTATATGCTTAGCAGCTTTTCCTTATCAAGGGAGCTCT | 60 |
| | <u>M I E V L L V T I C L A A F P Y Q G</u> <u>S S</u> | |
| | Presequence(signal peptide) | Prosequence |
| 61 | ATAATCCTGGAATCTGGGAATGTGAATGATTATGAAGTCGTGTATCCACGAAAGATCACT | 120 |
| | I I L E S G N V N D Y E V V Y P R K I T | |
| 121 | GCATTGTCCGAAGGAGCAGCTCAGCAAAAGTATGAAGATACCATGCAATATGAATTTAA | 180 |
| | A L S E G A A Q Q K Y E D T M Q Y E F K | |
| 181 | GTGAATGGAGAGCCGGTAGTCCTTCACCTGGAAAAAATAAAGAACTTTTTGCAAAAGAT | 240 |
| | V N G E P V V L H L E K N K E L F A K D | |
| 241 | TACAGCGAGACTCATTATTCCTTGATGGCACAAGAATTACAACATACCCCTCGGTTGAG | 300 |
| | Y S E T H Y S P D G T R I T T Y P S V E | |
| 301 | GATCACTGCTATTATCAGGGACGCATCCACAATGATGCTGACTCAACTGCAAGCATCAGT | 360 |
| | D H C Y Y Q G R I H N D A D S T A S I S | |
| 361 | ACGTGCAATGGTTTGAAAGGACATTTCAAGTTTCATGGGGAGAGGTACTTTATTGAACCC | 420 |
| | T C N G L K G H F K F H G E R Y F I E P | |
| 421 | TTGAAGCTTCCCGGCAGTGAAGCCCATGCAGTCTACAAATATGAAACATAGAAAAAGAG | 480 |
| | L K L P G S E A H A V Y K Y E N I E K E | |
| 481 | GATGAGACCCCCAAAATGTGTGGGGTAATCCAGAAATGGAAATCAGATGAGCTCATCAA | 540 |
| | D E T <u>P K M C G V</u> I Q K W K S D E L I K | |
| | Conserved sequence | |
| 541 | AAGCCCTTTCGGTTAAATCTTACTCCTCAACAACAAGAATCACCCCAAGCCAAGGTGTAC | 600 |
| | K P F R L N L T P Q <u>Q Q E</u> S P Q A K V Y | |
| | putative N-terminal(metalloproteinase domain) | |
| 601 | CTTGTCATAGTTGCGGATAAAAGCATGGTTGACAAACACAATGGTAATATAAAAAAGATA | 660 |
| | L V I V A D K S M <u>V D K H N G N I K K I</u> | |
| | CNBr-digestion | |
| 661 | GAAGAACAGGGACATCAAATGGTCAACACTATGAATGAGTGTTACAGACCTATGGGAATT | 720 |
| | <u>E E Q G H Q M V N T M N E C Y R P M G I</u> | |
| 721 | ATTATAATAATGGCTGGCATAGAATGTTGGACCACGAATGATTTCTTTGAAGTGAAGTCA | 780 |
| | I I I M A G I E C W T T N D F F E V K S | |
| 781 | TCAGCAAAAGAACTTTGTACTCATTTGCAAAATGGAGAGTAGAAGATTTGAGCAAGCGC | 840 |
| | S A K E T L Y S F A K W R V E D <u>L S K R</u> | |
| 841 | AAACCTCACAAATGATGCTCAGTTCCTCACGAACAAGGACTTCGATGGAAACACTGTAGGA | 900 |
| | <u>K P H N D A Q F L T N K D F D G N T V G</u> | |
| | Autoproteolytic fragment | |
| 901 | TTGGCTTTTGTGGGCGGCATATGCAACGAAAAGTATTGTGCAGGAGTTGTTTCAGGATCAT | 960 |
| | L A F V G G I C N E K Y C A G V V Q D H | |
| 961 | ACCAAAGTACCTCTTCTGATGGCAATTACAATGGGCCATGAGATCGGTCATAATCTGGGC | 1020 |
| | T K V P L L M A I T M G <u>H E I G H N L G</u> | |
| | Catalytic site | |
| 1021 | ATGGAACATGATGAAGCTAATTGTAAATGTAAAGCATGCGTTATGGCTCCCGAAGTAAAC | 1080 |
| | <u>M E H D</u> E A N C K C K A C V M <u>A P E V N</u> | |
| 1081 | AATAACCCAACCAAAAAGTTTCAGCGATTGTAGTAGGAATTATTATCAGAAGTTTCTTAA | 1140 |
| | <u>N N P T K K F S D C S R N Y Y Q K F L K</u> | |
| | CNBr-digestion | |
| 1141 | GATCGTAAACCAGAATGCTTGTTCAAGAAACCCTTGAGAACAGATACTGTTTCAACTCCA | 1200 |
| | D R K P E C L F K K P L R T D T V S T P | |
| 1201 | GTTTCTGGAAATGAACCTTTGGAGGTGATAACAATGGATGACTTCTATGCCTAA | |
| | V S G N E P L E V I T M D D <u>F Y A</u> * | |
| | putative C-terminal | |

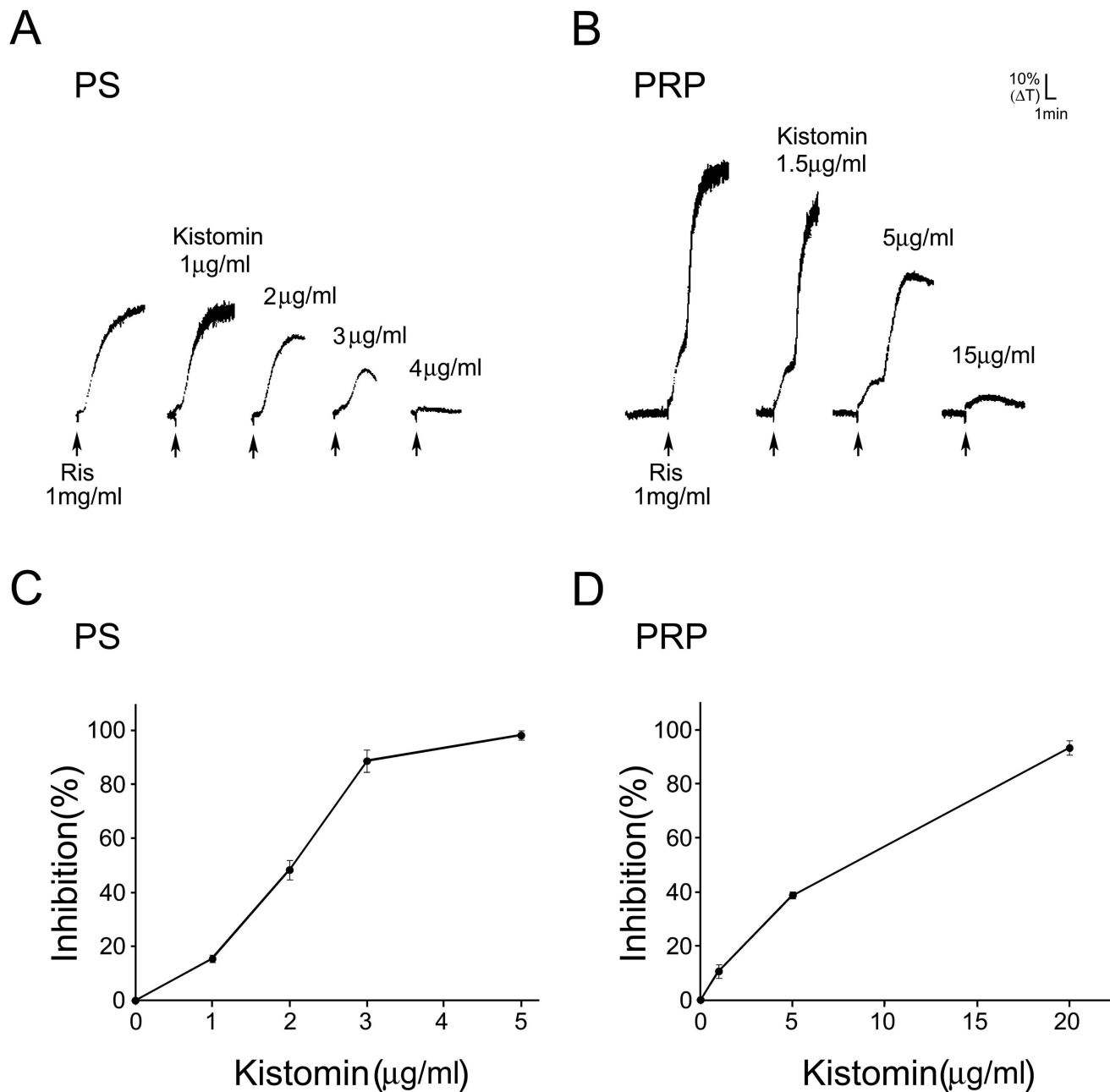
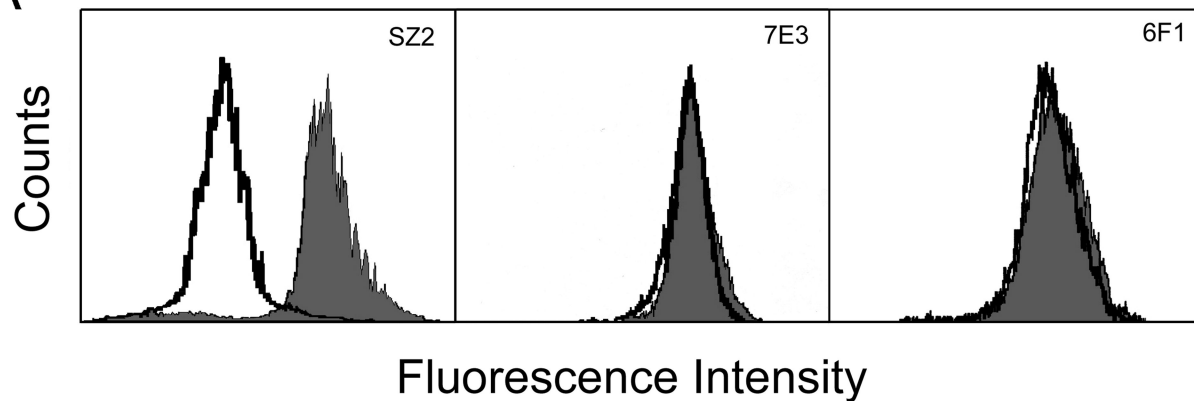


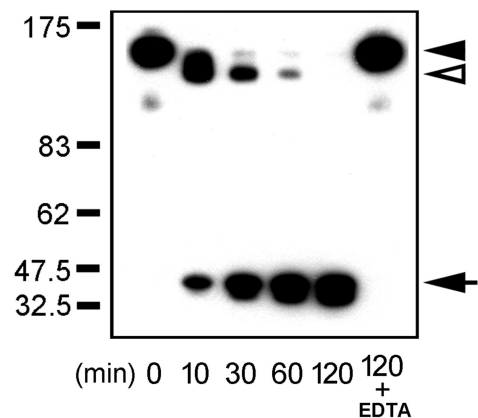
Figure3

MOL#38018

A



B



C

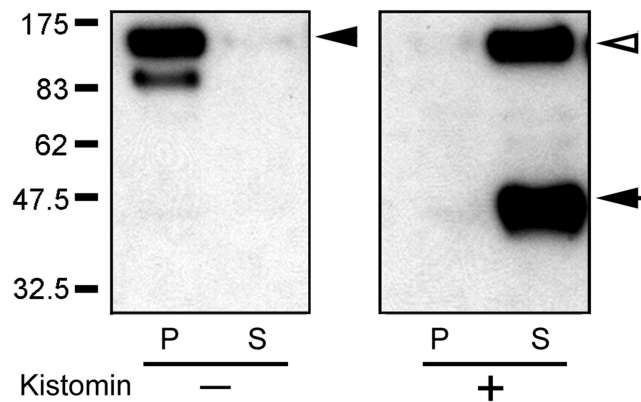
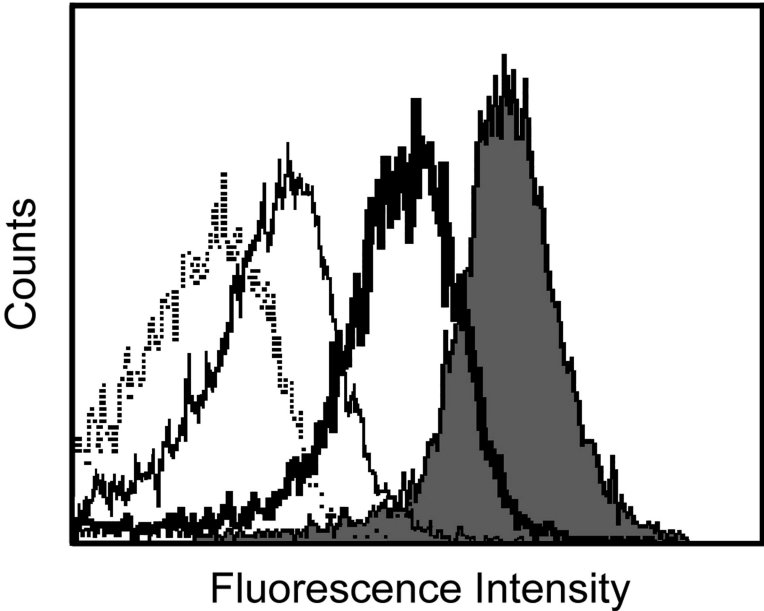


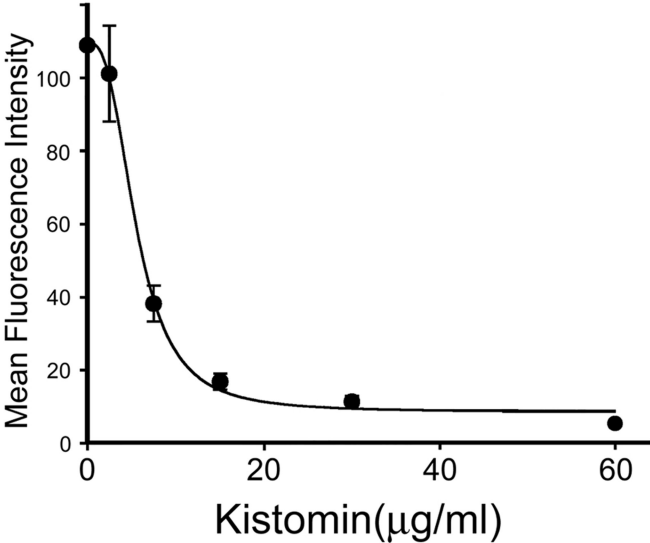
Figure4

MOL#38018

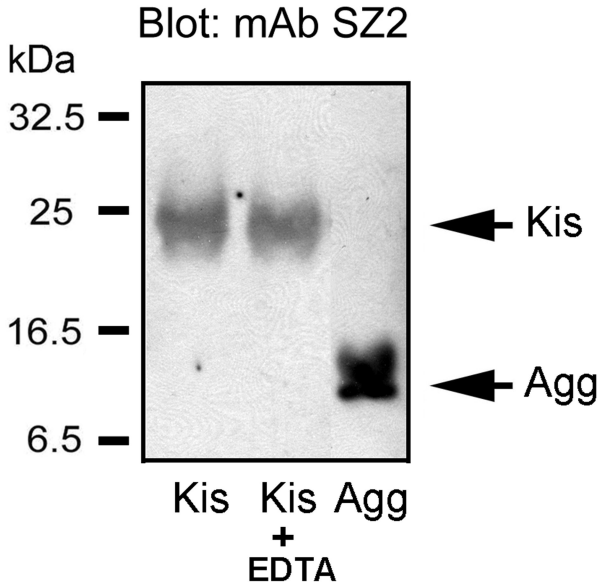
A



B



C



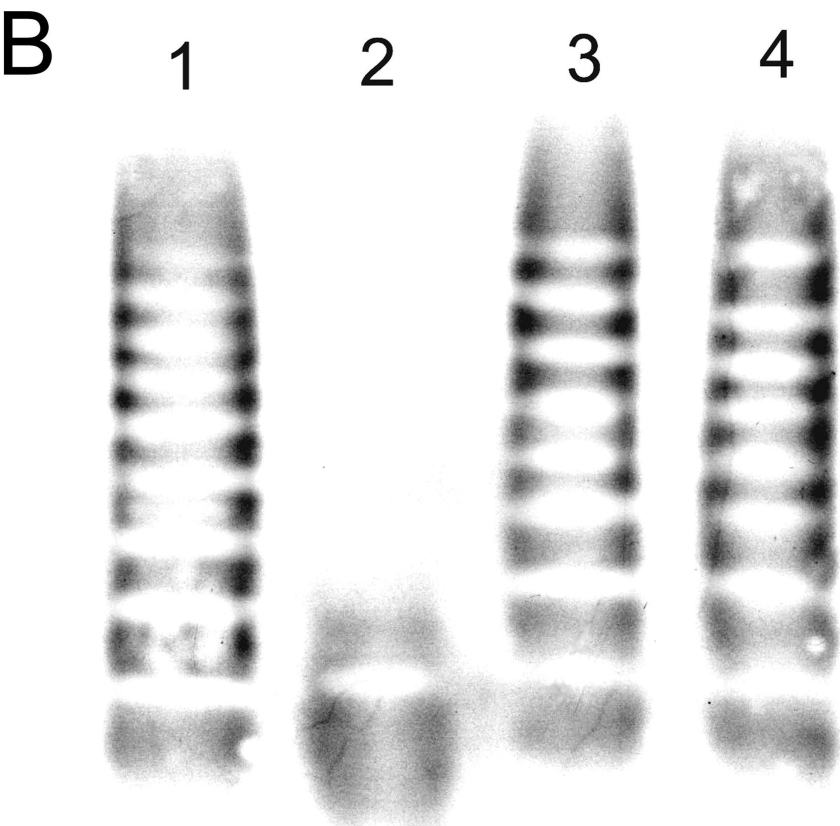
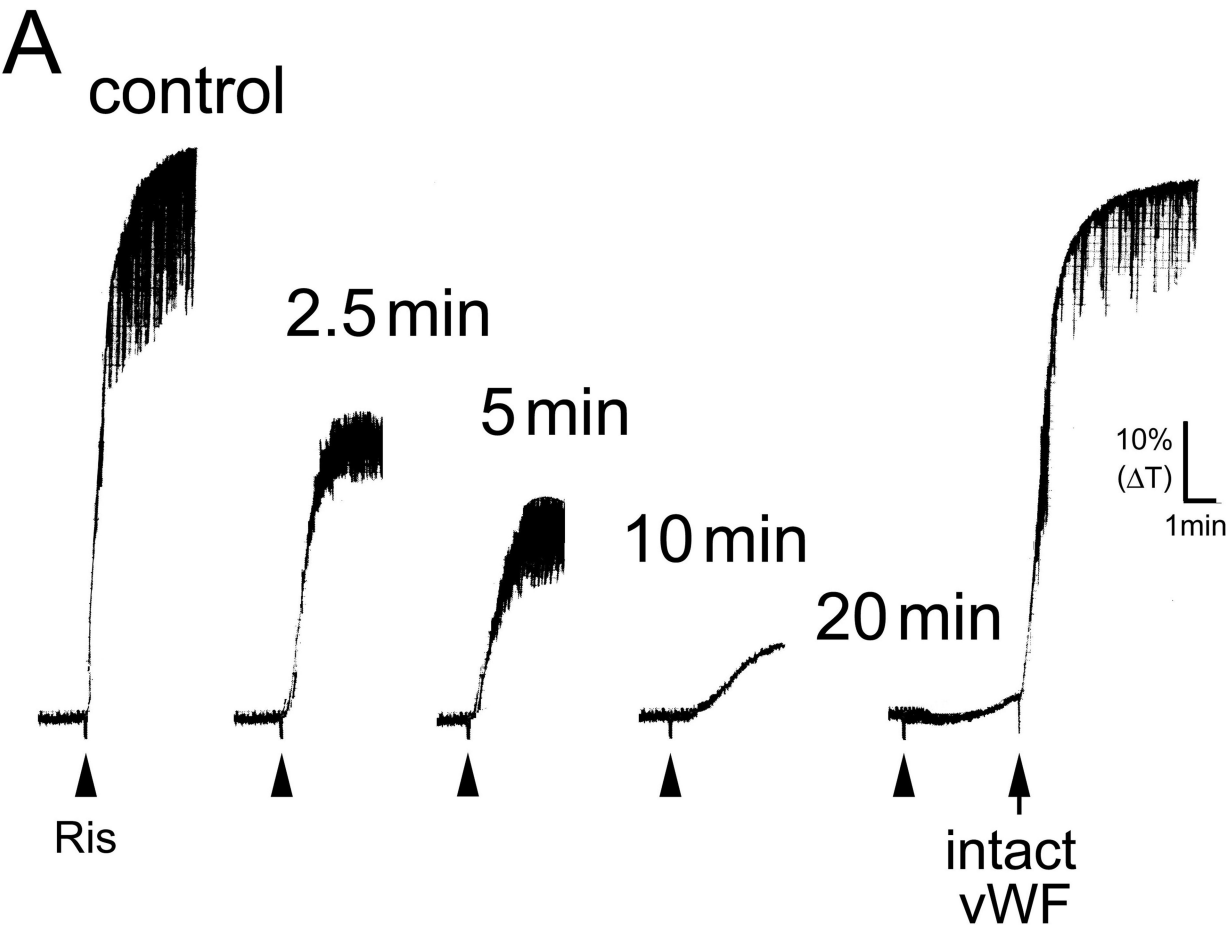


Figure6

MOL#38018

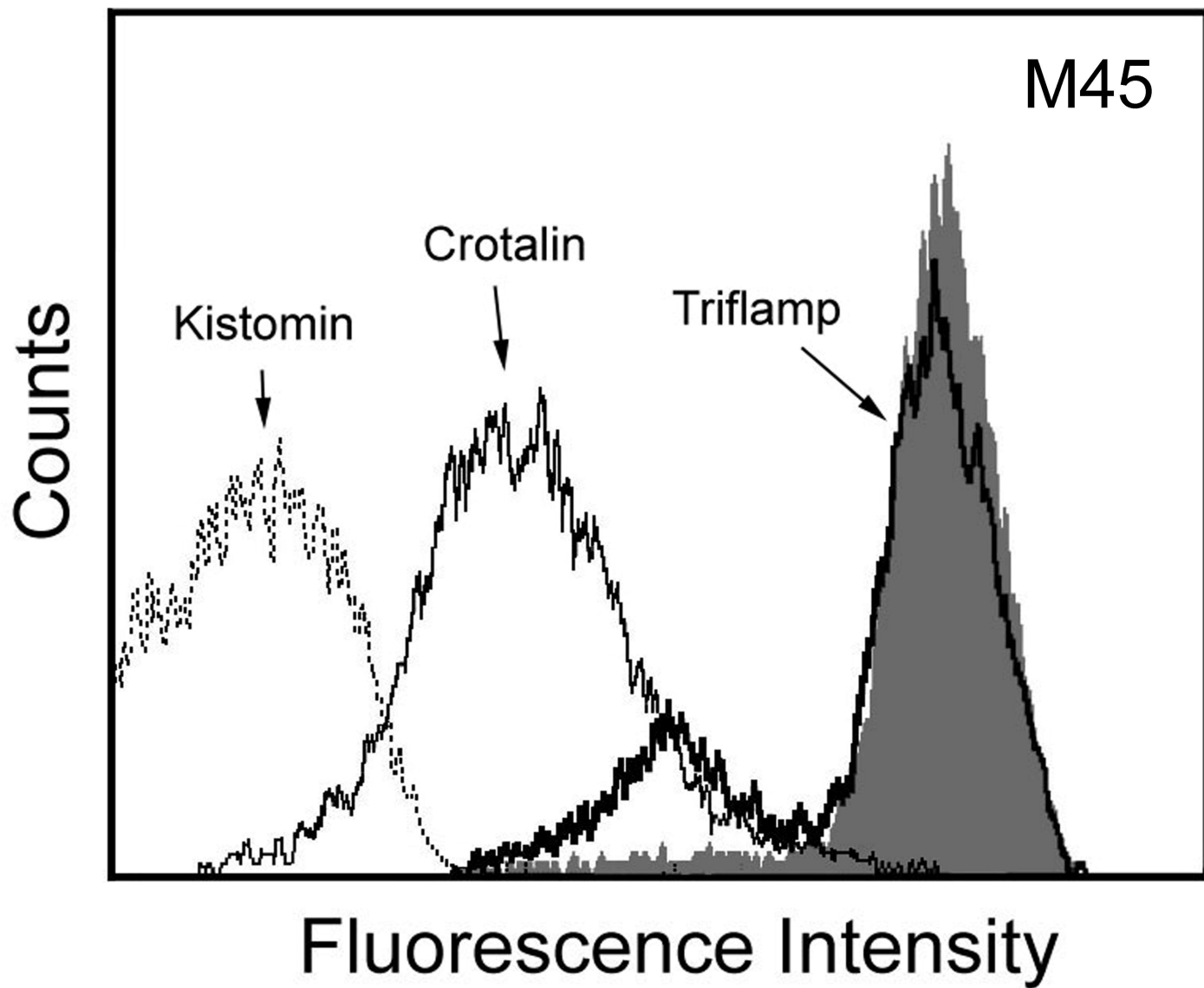


Figure7

MOL#38018

